CHAPTER

Size-exclusion chromatography

10

André M. Striegel
Chemical Sciences Division, National Institute of Standards and Technology, Gaithersburg, MD, United States

CHAPTER OUTLINE

10.1 INTRODUCTION

All synthetic, as well as most (or, at least, the most abundant) natural polymers possess a distribution of molar masses. As is the case for any statistical distribution, the molar mass distribution (MMD) is characterized by a series of averages or "moments."[1] The most common of these averages are the number-average, weight-average, and *z*-average molar mass, denoted as M_n, M_w, and M_z, respectively (and

[1] For an excellent discussion of the concept of statistical moments as it applies to the MMD of polymers, the reader is referred to Section 2.4 of Ref. [1].

Liquid Chromatography. http://dx.doi.org/10.1016/B978-0-12-805393-5.00010-5

defined mathematically via Eq. (10.22)). For a disperse (or polydisperse) polymer, $M_z > M_w > M_n$, whereas for monodisperse species, $M_z = M_w = M_n$. Discussion here will focus exclusively on the former scenario, in which case M_z is characteristic of the higher (larger molar mass) end of the MMD, M_n of the lower end, and M_w of an intermediate region near the mode. An example of this is seen in Fig. 10.1 for the monomodal MMD of a disperse, linear polystyrene (PS) homopolymer.

Because the z-average molar mass is usually located in a region of the MMD occupied by long chains, this average can inform knowledge of processing characteristics such as flex life and stiffness. Conversely, being located in the small-molecule region of the MMD, the M_n of a polymer can provide some idea as to the brittleness and flow properties of the material. Given the statistical nature of the various molar mass (M) averages, however, it is possible for polymers with very different MMDs to have identical M_n, M_w, M_z, and so on [2]. In addition, certain processing and end-use properties such as elongation, hardness, and yield strength may increase with increasing M, but decrease with a narrowing of the MMD. As such, examination of the MMD should almost always be performed in conjunction with an examination of

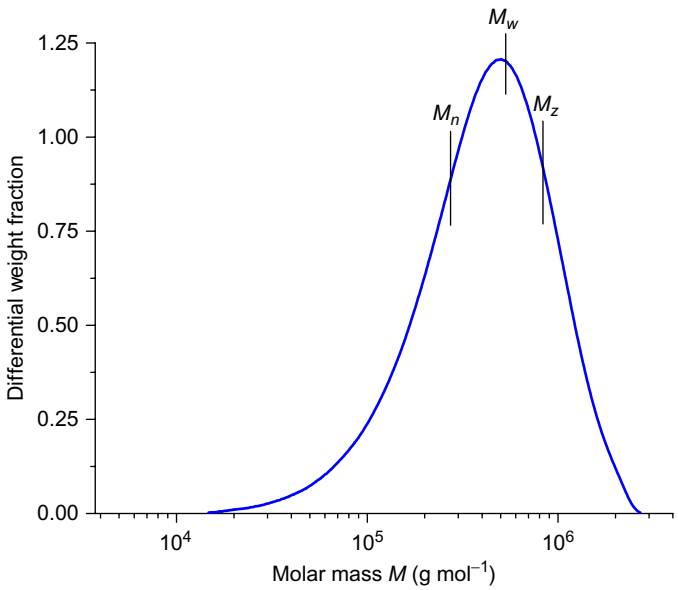

FIG. 10.1

Differential MMD and M averages of broad dispersity, linear PS. $M_n = 2.77 \times 10^5\,\mathrm{g\,mol^{-1}}$, $M_w = 5.38 \times 10^5\,\mathrm{g\,mol^{-1}}$, $M_z = 8.29 \times 10^5\,\mathrm{g\,mol^{-1}}$, and $M_w/M_n = 1.94$. Determined by SEC/MALS/DRI (*MALS*, multiangle static light scattering; *DRI*, differential refractometry) using a set of three PSS GRALlinear 10-μm particle size columns and one PSS GRAL10,000 10-μm particle size column, preceded by a guard column. Solvent: *N,N*-dimethyl acetamide + 0.5% LiCl; temperature: 35°C; flow rate: $1\,\mathrm{mL\,min^{-1}}$. Detectors: DAWN E MALS and Optilab DSP DRI. (A.M. Striegel, unpublished results).

the *M* averages of a polymer. The most common method for obtaining the MMD and accompanying averages, along with a host of other physicochemical polymer properties is, generally, size-exclusion chromatography (SEC).

10.2 HISTORICAL BACKGROUND

Many of the aforementioned relationships among macromolecular properties and the various *M* averages and/or the MMD were well-recognized by the early 1960s. However, no convenient method existed through which to determine the MMD and accompanying *M* averages of a polymer in a single experiment. To address this shortcoming, John Moore at the Dow Chemical Company, in Freeport, Texas, developed a technique he termed *gel permeation chromatography* (GPC). His paper, "Gel permeation chromatography. I. A new method for molecular weight distribution of high polymers" was published in 1964 [3].

The work of Moore built on earlier research by Wheaton and Bauman and by Porath and Flodin [4–6]. In 1953, the former researchers noted the fractionation of nonionic substances during passage through an ion-exchange column, which indicated that separation of molecules based on size should be possible in aqueous solution. This type of separation was demonstrated in 1959 by Porath and Flodin, who used columns packed with cross-linked polydextran gel, swollen in aqueous media, to effect the size-based separation of various water-soluble macromolecules. This aqueous-based technique became known as *gel filtration chromatography* (GFC). Although other hydrophobic gels were also developed for the separation of compounds of biological interest, the fact that the gels swelled only in aqueous media limited their application to water-soluble substances.

In his pioneering work, Moore used styrene/divinylbenzene gels cross-linked to a degree that balanced rigidity and permeability. Columns packed with these gels were connected to a differential refractometer (DRI), specially designed by James Waters with an optical cell smaller than what was commercially available at the time, with continuous flow in both the sample and reference sides of the cell, and capable of operating at temperatures up to 130°C [7]. Moore recognized that, with proper calibration, GPC could provide both the MMD and *M* averages of synthetic polymers, a capability which was quickly capitalized on by many scientists in the polymer industry, who had been longing for just such a technique. In the words of A. C. Ouano, "With the introduction of GPC by Moore, molecular weight distribution data for polymers took a sudden turn from near nonexistence to ready availability" [8]. The early history of the instrumental development and commercialization of GPC by Waters Corp. is elegantly recounted in the articles by McDonald [9,10].

We reconcile at this point in the chapter the terms GPC and GFC under the common term SEC. There are a number of good reasons for doing this: First, elution in both GPC and GFC proceeds by a common size-exclusion mechanism. Second, whereas many SEC columns are still packed with cross-linked gels, just as many

are packed with "nongel" materials such as porous silica and alumina and, more recently, monoliths. Finally, because GPC was the term used when operating in organic solvents, whereas GFC denoted experiments in an aqueous medium, it is difficult to avoid pointing out that a particular researcher might perform GPC experiments on a Monday and GFC experiments on a Friday of the same week, using the exact same hardware (and, perhaps, even the same columns), and separating analytes via the same chromatographic mechanism, only using a different solvent. Because of these reasons, the all-inclusive and more aptly descriptive term SEC is preferred and used from here onward.

The column packings used both by Moore and by Porath and Flodin were lightly cross-linked, semirigid networks of large (≈75–150 μm) particles that could be used only at low flow rates and operating pressures (<250 psi, or 1.7 MPa), resulting in long, relatively inefficient analyses. The introduction, in the 1970s, of μ-Styragel, which consisted of semirigid 10 μm cross-linked PS particles capable of withstanding pressures of several thousand psi, simultaneously allowed for both faster analysis and superior performance compared with what had been previously possible. Since then, a variety of packing materials have been introduced, ranging in size from around 3–20 μm and capable of separating anywhere from monomers and oligomers to ultrahigh-*M* polymers and, even, particles.

In the intervening decades, advances in SEC have been guided mostly by the need for absolute (i.e., calibrant-independent) *M* determination, by a multidetector approach aimed at determining physicochemical distributions and heterogeneities, and by the incorporation of SEC into two-dimensional liquid chromatographic (2D-LC) scenarios to further the understanding of complex polymers and blends. These topics will be treated in Sections 10.6 and 10.7. First, however, we review some of the fundamental chromatographic principles of SEC.

10.3 RETENTION IN SEC

"Retention in SEC is an equilibrium, entropy-controlled, size-exclusion process" [2]. This statement merits some attention, and each part of it will be examined individually here, in the reverse order.

10.3.1 A SIZE-EXCLUSION PROCESS

Let us suppose we inject a disperse analyte (e.g., the PS in Fig. 10.1), or a mix of narrow dispersity analytes, onto an SEC column which is packed with an inert, porous substrate. Due to their size, the larger component of the analyte or mix will sample either a smaller number of pores or/and, within a given pore, smaller pore volume than will the smaller components of the sample. Because of this behavior, the larger components will elute from the column first and the smaller components will elute later. Elution in SEC is in the reverse order of the analyte size, and the method may be thought of as an "inverse-sieving" technique.

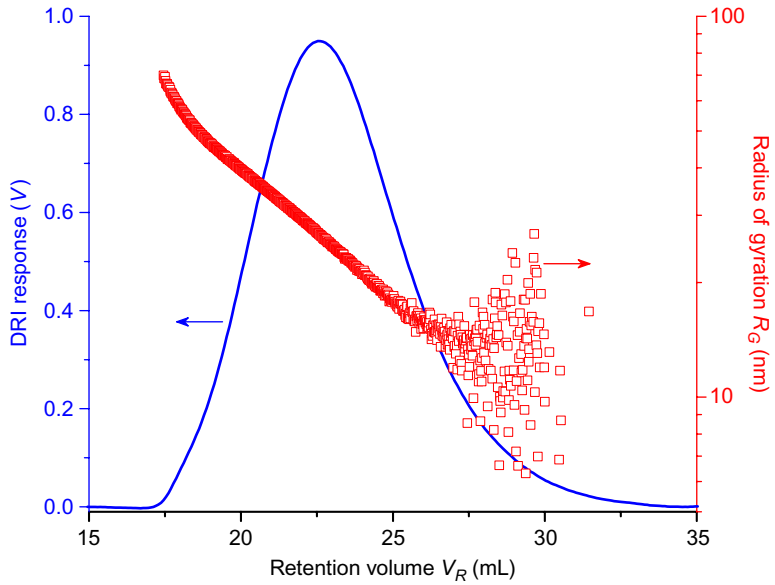

FIG. 10.2

SEC chromatogram as monitored by differential refractometer, DRI (*solid blue line*), and radius of gyration versus retention volume relationship (*open red squares*), of PS sample in Fig. 10.1. Experimental conditions same as in the legend for Fig. 10.1. Scatter in R_G when $V_R > 27$ mL corresponds to molecules with insufficient angular dissymmetry, at experimental conditions, to allow for accurate measurement of R_G; see Section 10.6 for details.

Do samples actually behave in the manner described above? Fig. 10.2 shows that the size (as exemplified here by the radius of gyration[2]; see Section 10.6) of the broad dispersity PS in Fig. 10.1 decreases steadily as retention volume increases, that is, the sample eluted by a size-exclusion process. An abundance of similar examples can be found in the literature, including almost any SEC calibration curve in which narrow dispersity standards are observed to elute in order of decreasing M (for a homologous series at a given set of solvent/temperature conditions, $M \propto$ size).

10.3.2 AN ENTROPY-CONTROLLED PROCESS

For dilute solutions at equilibrium (the equilibrium nature of SEC is examined next), solute distribution is related to the standard free-energy difference ($\Delta G°$) between the phases at constant temperature and pressure:

$$\Delta G° = -RT \ln K \tag{10.1}$$

[2] It should be noted that a quantitative relationship has not yet been established between the solvated volume occupied by the analyte in solution and any main macromolecular radius, such as the radius of gyration R_G. For a more detailed discussion, the reader is referred to Section 2.6.2 of Ref. [2].

with

$$\Delta G^\circ = \Delta H^\circ - T\Delta S^\circ, \tag{10.2}$$

where K is the solute distribution coefficient, R the gas constant, T the absolute temperature, and ΔH° and ΔS° are the standard enthalpy and entropy differences between the phases, respectively.

In "traditional" LC (e.g., normal- and reversed-phase LC), retention is generally governed by solute-stationary phase interactions, sorptive or otherwise, and solute transfer between phases is associated with large enthalpy changes. In SEC, noninteracting (hopefully) column packing materials are used, corresponding to $\Delta H^\circ \approx 0$, and it is the change in entropy between phases that governs solute retention, as per:

$$K_{SEC} \approx e^{\Delta S^\circ / R}, \tag{10.3}$$

where K_{SEC} is the solute distribution coefficient in SEC, corresponding to the ratio of the average solute concentration inside the pores of the column packing material to the concentration outside the pores. Because solute mobility is more limited inside than outside the pores, solute permeation in SEC is associated with a decrease in solution conformational entropy, corresponding to the negative values of ΔS°.

Eq. (10.3) predicts that solute retention in SEC should be temperature-independent. Although it is realized that the size of polymers in solution and, hence, their SEC retention volume, has a modest temperature dependence (and, sometimes, a larger dependence, as when transitioning through the theta point of the solution), this does not affect the mechanism by which these analytes elute. The entropic nature of SEC retention has been confirmed by noting the virtual lack of change in K_{SEC} with changes in temperature for a large number of mono-, di-, and oligosaccharides in both aqueous and nonaqueous systems [11–15]. Some of these data are given in Table 10.1.

It is a truism that there will be enthalpic contributions to all real SEC separations; it is only the magnitude of these contributions which will differ. In certain specialized

Table 10.1 Temperature Independence of K_{SEC}

	K_{SEC}	
Oligosaccharide	**25°C**	**37°C**
Maltose	0.683	0.675
Maltoheptaose	0.430	0.415
Cellobiose	0.657	0.648
Cellopentaose	0.431	0.419
Isomaltose	0.626	0.613
Isomaltoheptaose	0.356	0.341
Laminaribiose	0.657	0.643
Laminariheptaose	0.369	0.354

Solvent: H_2O, pH: 7.4, flow rate: 1 mL min^{-1}. Columns: Four Ultrahydrogel 6 μm-particle size, 120 Å pore size; detector: Optilab rEX. See Refs. [13,15] for details.

cases, such as when using SEC to calculate the ΔS of monodisperse analytes in solution, it is essential that $\Delta H \approx 0$. As seen in Table 10.1, this can be verified by varying the temperature of the experiment and noting that, if the enthalpic contribution is small then, with a relatively large (≈10–20°C, or more) change in temperature, K_{SEC} will change by only a few percent. Even in nonspecialized cases, a large ΔH component of the separation should be avoided, as this may cause coelution due to some of the smaller components in a sample eluting by an entropically dominated process whereas the elution of larger components reflects a substantial enthalpic contribution to their separation.

10.3.3 AN EQUILIBRIUM PROCESS

The thermodynamic equilibrium of the SEC retention process has been confirmed through two independent sets of experiments. The first set demonstrated that the solute distribution coefficient is independent of the flow rate, over a flow rate range of approximately one order of magnitude and a molar mass range of approximately three orders of magnitude, for two different types of analytes, narrow dispersity PS and poly(methyl methacrylate) (PMMA) standards [2,16]. Results for the latter are shown in Fig. 10.3, demonstrating that retention in SEC is governed by the *extent* of analyte permeation into the pores of the column packing material, not by the *rate* of permeation. It should be noted that, 40 years earlier, James Waters and colleagues found the retention volume of both solvent tracers and large polymeric analytes to be essentially flow rate-independent for flow rates spanning two orders of magnitude using, individually, columns of three different particle sizes [17].

The second set of experiments confirming the thermodynamic equilibrium of SEC retention compared results from flow and static mixing experiments for a set of narrow dispersity PS standards covering approximately three orders of magnitude in M [2,18,19]. In the flow experiments, solute distribution coefficients were calculated from the experimentally measured retention volumes of the analytes, V_R, and interstitial (total exclusion) and pore volumes of the column, V_o and V_p, respectively, as per:

$$K_{SEC} = \frac{V_R - V_o}{V_p} \tag{10.4}$$

In the static mixing experiments, polymer solutions of known volume and initial concentration C_i were mixed with a known amount of dry, porous packing material. The mixture was allowed sufficient time for complete solute permeation, and the concentration C_o of the final solutions was then measured and compared with C_i. The change in the concentration of the solutions provides a direct measure of equilibrium solute distribution. If solute retention in SEC is really an equilibrium process, then the K_{SEC} values determined by the flow experiments should vary linearly with the corresponding values $1–C_i/C_o$ obtained from the static mixing experiments. This is exactly the behavior observed in Fig. 10.4.

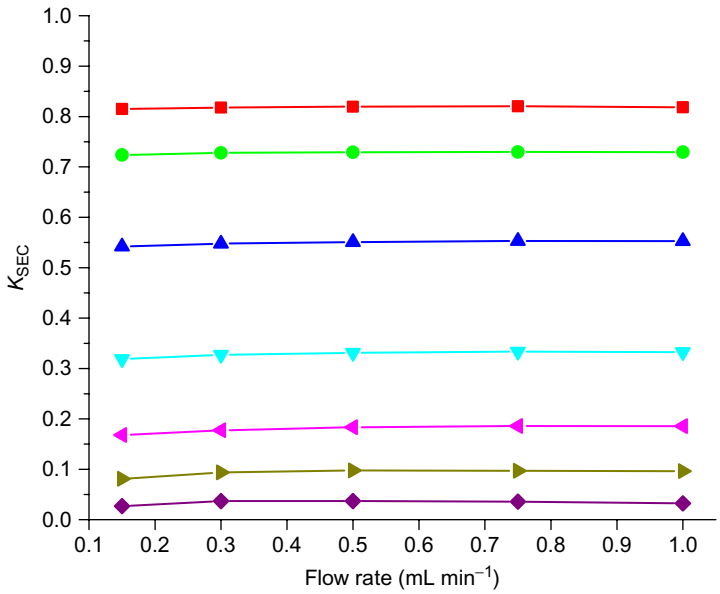

FIG. 10.3

Flow rate independence of K_{SEC}. Narrow dispersity linear PMMA standards in tetrahydrofuran (THF) at 30°C, with peak-average molar mass M_p in g mol^{-1} of (■) 1.27×10^3, (●) 4.91×10^3, (▲) 2.70×10^4, (▼) 1.07×10^5, (◀) 2.65×10^5, (▶) 4.67×10^5, (◆) 8.38×10^5. Results are averages of triplicate injections. In all the cases, standard deviations are substantially smaller than data markers and, therefore, not shown. *Solid lines* are placed on graph to guide the eye and are not meant to imply continuity between data points. Column: One 7.5 mm × 300 mm PLgel 10-μm particle size, 10^4 Å pore size; detector: Optilab rEX DRI. See Section 10.2.4 of Ref. [2] for a more extended discussion, and Ref. [16] for experimental details.

Adapted from Striegel AM, Yau WW, Kirkland JJ, Bly DD. Modern size-exclusion liquid chromatography. 2nd ed. New York: Wiley; 2009.

10.4 BAND BROADENING IN SEC

The various possible contributions to column band broadening in SEC are expressed in the expanded van Deemter equation [2]:

$$H = A + \frac{B}{v} + C_M v + C_{SM} v + C_S v \tag{10.5}$$

where H is the plate height, v is the flow velocity, A is the contribution to band broadening from eddy dispersion, B is the contribution from longitudinal diffusion, C_M is the contribution from mobile-phase mass transfer processes (extraparticle processes occurring in the interstitial medium, as they affect band broadening but not as they

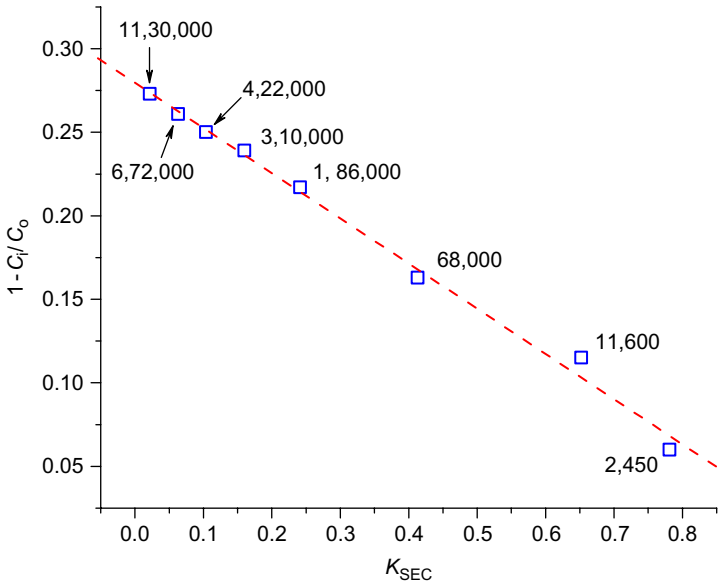

FIG. 10.4

Static mixing data versus equilibrium solute distribution in SEC. Abscissa (K_{SEC}) values from flow-mode SEC experiment, ordinate ($1–C_i/C_o$) values from static mixing experiment. PLgel 10-μm particle size, 10^4 Å pore size column packing material from the same manufacturer was used in both sets of experiments. Samples: 0.1% PS in THF. For static mixing experiments, 10 mL of solution was mixed with 2 g of porous stationary phase. Each point represents the average of triplicate measurements, with standard deviations along both axes substantially smaller than data markers and, therefore, not shown. *Dashed red line* represents first-order nonweighted linear fit to the data ($r^2=0.994$). Numbers next to data markers represent M_p, in $g\,mol^{-1}$, of each narrow dispersity linear PS standard. See Ref. [19] for details.

Reprinted with permission from Striegel AM. Thermodynamic equilibrium of the solute distribution in size-exclusion chromatography. J Chromatogr A 2004;1033:241–5.

effect retention by alternative mechanisms, for example, hydrodynamic chromatography [20–22]), C_{SM} is the contribution from stagnant mobile-phase mass transfer processes (because the nonflowing solvent inside the pores of the column packing material is the actual stationary phase in SEC, the C_{SM} term in SEC is often referred to as "stationary phase mass transfer"), and C_S is the contribution from traditional LC sorption-desorption processes.

Eq. (10.5) bears some examination. First, as discussed in the previous section, in most SEC experiments the enthalpic contribution to retention is minimal, which corresponds to $C_S \approx 0$. Second, as seen in Fig. 10.5A, stop-flow experiments have demonstrated that, for nonoligomeric (i.e., large-M) analytes at analytical flow rates (e.g., $\approx 1\,mL\,min^{-1}$), longitudinal diffusion effects are minimal ($B \approx 0$) though, as seen in Fig. 10.5B, this is no longer true in the case of oligomeric SEC or when using very low

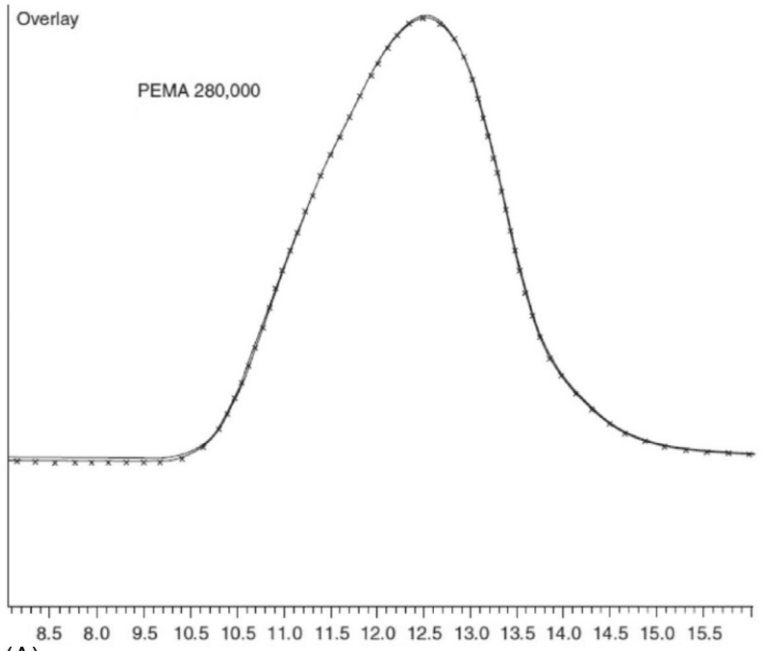

(A)

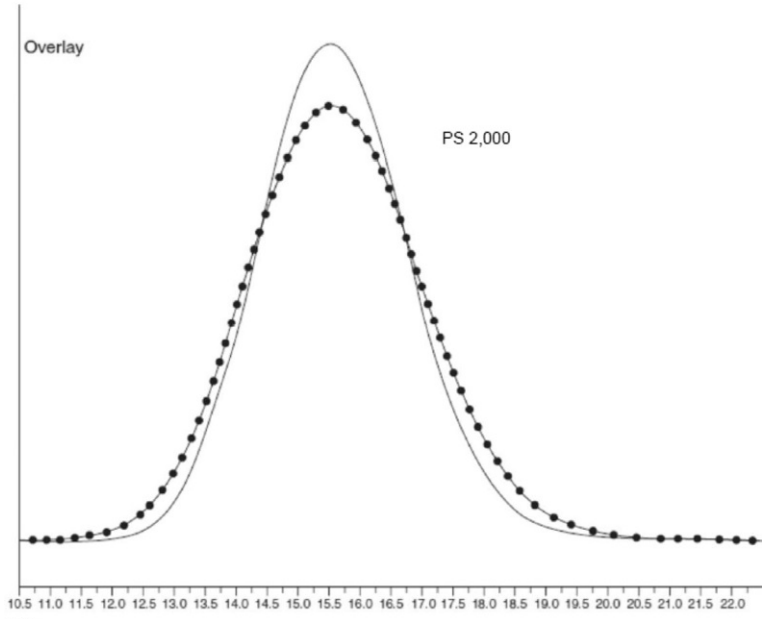

(B)

FIG. 10.5

Stop-flow study of longitudinal diffusion in SEC. Figures show retention volume versus DRI response, with solid curves corresponding to "normal" injection and elution (i.e., uninterrupted flow at $1\,mL\,min^{-1}$) and *crossed or dotted curves* corresponding to elution after abruptly halting flow and then holding analytes on-column for 16 h. (A) $280{,}000\,g\,mol^{-1}$ poly(ethyl methacrylate), PEMA and (B) $2000\,g\,mol^{-1}$ PS. Solvent: THF; temperature: 35°C; flow rate during elution: $1\,mL\,min^{-1}$; columns: PLgel 5-μm particle size mixed-C; detector: HP 1037A DRI.

Reprinted with permission from Striegel AM. Longitudinal diffusion in size-exclusion chromatography: a stop-flow size-exclusion chromatography study. J Chromatogr A 2001;932:21–31.

flow rates (e.g., ≈0.1 mL min^{-1}) [23]. These low flow rates are oftentimes needed to prevent on-column, flow-induced degradation of large, ultrahigh-*M* analytes [24–27].

A consequence of Eq. (10.5) is that H is expected to increase linearly with flow velocity v at high flow rates. However, this is not what has been observed experimentally. Rather, it has been found that plate height tapers off at high flow rates. The observed behavior appears to be a consequence of flow-diffusion coupling, as first proposed by Giddings. In Giddings' coupling theory (explained completely in Refs. [28] and [29] and, as it applies to SEC, in Section 3.2.3 of Ref. [2]), the effects of eddy diffusion (A term) and mobile-phase mass transfer (C_M term) combine to provide more chances for each solute molecule to experience the different velocities in the various flow channels. If individual molecules can sample the various streamlines of flow with increased frequency, then there is a higher probability that the molecules will attain the same statistical mean velocity as each other and elute from the columns closer together, thus reducing band broadening. This combined mobile-phase plate height is given the term H_M and can be expressed as

$$H_M = \frac{1}{\frac{1}{A} + \frac{1}{C_M v}} \tag{10.6}$$

As a result of the above discussions regarding C_S, B, and the coupling of A and C_M, *for nonoligomeric analytes at analytical flow rates*, we can write the approximate expression:

$$H_{\text{SEC}} \approx C_{SM} v + \frac{1}{\frac{1}{A} + \frac{1}{C_M v}} \tag{10.7}$$

If one wishes to compare the band broadening characteristics of two or more columns, each packed with particles of different sizes, then it is necessary to express plate height and flow velocity as the dimensionless quantities "reduced plate height" **h** and "reduced velocity" **v**, defined as per:

$$\mathbf{h} = \frac{H}{d_p} \tag{10.8}$$

$$\mathbf{v} = \frac{v d_p}{D_M} \tag{10.9}$$

where d_p is the average diameter of the column packing particles (expressed in the same units as H), and D_M is the solute translational diffusion coefficient in the interparticle space or in the free solution (expressed in units that will make **v** dimensionless).

10.4.1 EXTRA-COLUMN EFFECTS

Band broadening results not only from diffusive processes within the chromatographic column, but also from dispersion which can occur at several locations outside

the column. The latter include the sample injector, detector cell, column-end fittings, connectors, and so on. The total band width measured, W_t, is thus a function of the kinetic, van Deemter-type column processes discussed above, denoted as W_c, with a contribution W_i from the sample injection volume, and additional contributions W_d, W_j, and W_x from, the detector, end fittings, and connecting tubing, respectively. The relationship between these terms can be expressed as

$$W_t^2 = W_c^2 + W_i^2 + W_d^2 + W_j^2 + W_x^2 \tag{10.10}$$

W_c can be minimized by judicious application of the rate theoretical concepts discussed above, which allow determination of the optimal flow velocity at which plate height will be minimal, thus maximizing plate number and optimizing column efficiency. Minimizing extra-column dispersion is beyond the scope of this chapter, but is discussed in detail in Chapter 5 of Ref. [2]. As a thumb rule, however, achieving the following will only increase W_t by $\approx 10\%$ over the contribution from W_c:

$$\left(W_i + W_d + W_j + W_x\right) < \frac{W_c}{3} \tag{10.11}$$

where W_c is measured for the peak of a monodisperse (or narrowly dispersed) analyte.

10.5 RESOLUTION IN SEC

Resolution provides a measure as to how well two eluted bands are separated from each other. It is given the symbol R_s and defined as

$$R_s = \frac{2\left(V_{R2} - V_{R1}\right)}{W_{b1} + W_{b2}} \tag{10.12}$$

where 1 and 2 denote the two individual bands and W_b is the peak width at the base of the chromatogram (formed by the intersection of the tangents to the peak inflection points with the baseline). In general, $W_b = 4\sigma$, where σ is the peak standard deviation.

Although Eq. (10.12) serves to *describe* resolution, it does not provide insight into how to *improve* resolution. The latter can be obtained from Eq. (10.13) [30]:

$$R_s = \frac{\sqrt{N}}{4}\left(\frac{\alpha - 1}{\alpha}\right)\left(\frac{k}{1 + k}\right) \tag{10.13}$$

where the *separation factor* α is defined as $\alpha = K_{D2}/K_{D1} = k_2/k_1$ (where K_D is the solute distribution coefficient, K_{SEC} in an SEC experiment); the *retention factor* k is defined as $k = (K_D V_s/V_m)$, where V_s and V_m are, respectively, the volumes of stationary and mobile phases; and N is the plate number of the column, defined as $N = L/H$, with L being the column length. Eq. (10.13) has been referred to as the *fundamental resolution equation in chromatography* and its derivation can be found in standard separation science textbooks (e.g., Ref. [31]). It reconciles the thermodynamics and kinetics of separations, the former via the α and k terms, the latter via N. Because these three terms can be adjusted somewhat independently of each other, an examination of

Eq. (10.13) shows how column resolution can be optimized by effecting changes in column length (or number of columns), flow rate, temperature, and choice of stationary phase (both size and chemistry) and mobile-phase. Rearrangement of this equation also allows for the calculation of the number of plates needed to realize a separation with a given resolution, and also of the time required to elute two solutes with a given resolution.

It should be noted that, of the parameters that can be adjusted to optimize R_s, only column length (or number of columns), flow rate, and size of the column packing material are normally adjusted in SEC. Further limitations are imposed in the case of large, ultrahigh-M macromolecules, which have the potential to degrade during passage through the column packing material as a result of the large strain rates that can develop in packed bed. In such cases, low flow rates and large-sized packing materials are often used, thus sacrificing resolution for the sake of sample integrity.

The quantitative description of resolution in SEC builds on Eq. (10.12) and on the dependence of SEC peak separation ΔV_R on solute molar mass, where the latter relation can be obtained by constructing a calibration curve. For two molecules, 1 and 2, of the same type of polymer but differing from each other by a molar mass factor M_2/M_1, resolution can be written as [2]

$$R_s = \frac{\ln\left(M_2 / M_1\right)}{2D_2\left(\sigma_1 + \sigma_2\right)} \approx \frac{\Delta \ln M}{4D_2\sigma} \tag{10.14}$$

where σ is the peak standard deviation and D_2 is the slope of the calibration curve. In SEC, interest is less in the resolution between a specific pair of analytes and more in resolution as it pertains to the elution curve as a whole. To this effect, the concept of *specific resolution* R_{sp} was developed, which eliminates the dependence of R_s on M [2,32]:

$$R_{sp} = \frac{R_s}{\Delta \log M} = \frac{0.58}{D_2\sigma} \tag{10.15}$$

Finally, introduction of the term R_{sp}^{*} allows comparison of the resolution of columns of different lengths, or among column sets comprised of different numbers of columns. Because $D_2 \propto 1/L$, whereas $\sigma \propto L^{1/2}$, normalizing the column length out of the specific resolution equation gives [2,32]

$$R_{sp}^{*} = \frac{0.58}{D_2\sigma\sqrt{L}} \tag{10.16}$$

10.6 SEC ENTERS THE MODERN ERA: THE DETERMINATION OF ABSOLUTE MOLAR MASS

The introduction of rigid and semirigid columns packing materials capable of withstanding high pressures marked a change in how SEC was performed, in that it allowed for reduced analysis times and increased column efficiencies. Nonetheless, molar mass averages and distributions were still obtained by applying calibration curves constructed using sets of relatively narrow dispersity standards (or, occasionally, well-characterized

Table 10.2 Difference Between M_w Values (in g mol^{-1}) Obtained Using a Single DRI Detector and Applying a Linear PS-Based Calibration Curve, Versus Using an Online MALS Detector

Sample	SEC/PS-Relative[a]	SEC/MALS[b]
PMMA	74,000	87,000
PS 3-arm star	178,000	249,000
PS 8-arm star	58,000	77,000
PVAc	220,000	367,000

[a] Values obtained using a set of three PLgel 5 μm particle size Mixed-C columns operating in THF at 35°C and applying a third-order calibration curve. DRI vacuum wavelength of operation: 940 nm. Calibrants: Narrow dispersity linear PS standards in the Mp range of 162 g mol^{-1} to 1.13×10^6 g mol^{-1}, inclusive.
[b] Experimental conditions same as those in the legend for Fig. 10.1.
From Striegel AM, Yau WW, Kirkland JJ, Bly DD. Modern size-exclusion liquid chromatography. 2nd ed. New York: Wiley; 2009.

broad standards) and using systems consisting of a single, concentration-sensitive detector, most commonly a DRI. In most cases, the standards bore little, if any, chemical and/or architectural resemblance to the analytes themselves. The lack of accuracy of this type of approach is reflected in the results in Table 10.2, as discussed in the next paragraph. As we shall soon see, SEC with online multiangle static light scattering detection (SEC/MALS) can be considered a benchmark approach to obtaining M averages and distributions. To results from SEC/MALS we compare results obtained by SEC/DRI (i.e., with only a DRI detector connected to the SEC columns), applying a calibration curve constructed using well-characterized, narrow dispersity linear PS standards.

Not shown in Table 10.2 are results for both broad and narrow MMD linear PS samples. For these, which are samples with the same chemical repeat unit and architecture as the calibrants, accurate and precise M averages and distributions are obtained via SEC/DRI applying the calibration curve constructed using PS standards analyzed at the same experimental conditions as the samples. However, if the chemical identity of the sample is different from that of the calibrants, as is the case with the PMMA sample in Table 10.2, even though they are both linear polymers, the different hydrodynamic volumes occupied by a PS and a PMMA polymer of the same M result in an error in the M determined by applying the PS-based calibration curve. Errors in calculated M are also seen when the chemistry, but not the architecture, of the analyte is the same as that of the calibrants. This is the case for the 3-arm and the 8-arm star polystyrenes in Table 10.2. In the case of the poly(vinyl acetate) (PVAc) sample for which data are given in the table, which is a polymer with random long-chain branching, both the chemistry and architecture of the analyte differ from those of the calibrants, resulting in a 40% error in calculated M_w!

10.6.1 UNIVERSAL CALIBRATION AND ONLINE VISCOMETRY

In their landmark 1967 paper entitled "A universal calibration for gel permeation chromatography" [33], Grubisic, Rempp, and Benoit demonstrated how a plot of

retention volume versus the logarithm of the product of intrinsic viscosity and molar mass (i.e., a plot of V_R versus $\log\{[\eta]\times M\}$) produced a calibration curve (such as that shown in Fig. 10.6 for linear PS and PMMA [34]) that was independent of calibrant chemistry and architecture.[3] The consequence of this was that, if a universal calibration curve was constructed with readily available, well-characterized standards such

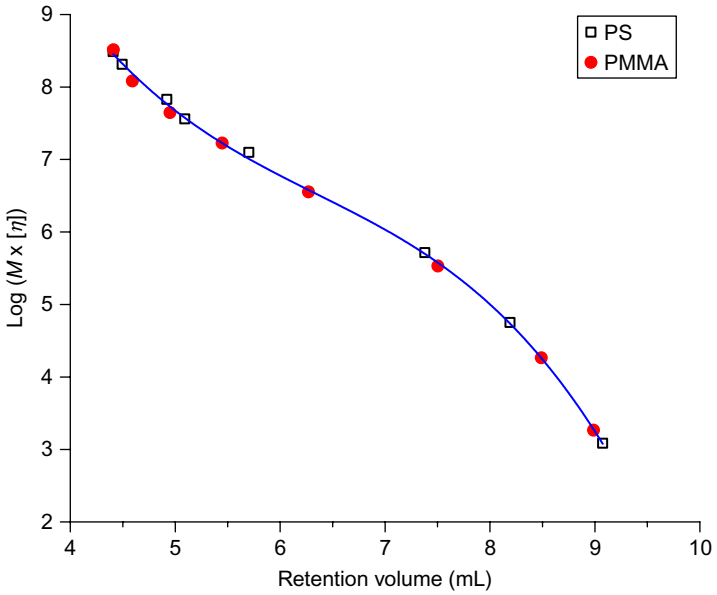

FIG. 10.6

Universal calibration plot of narrow dispersity linear PS and PMMA standards. For PS, represented by open black squares (□), peak-average molar masses (M_p) of the standards, in g mol^{-1}, are 9.25×10^2, 8.45×10^3, 3.03×10^4, 1.89×10^5, 3.50×10^5, 5.00×10^5, and 9.50×10^5. For PMMA, represented by *filled red circles* (●) the M_p in g mol^{-1} are 1.28×10^3, 4.91×10^3, 2.70×10^4, 1.07×10^5, 2.65×10^5, 4.67×10^5, and 8.38×10^5. Each data point represents the average of at least triplicate determinations, with standard deviations substantially smaller than point makers (therefore not shown). *Solid blue line* represents the universal calibration curve obtained via a nonweighted third-order fit to the data points, with $r^2=0.999$. Determined using a PLgel 10-μm particle size, 10^4 Å pore size column. Solvent: THF; temperature: 30°C; flow rate: 1 mL min^{-1}.

Adapted from results presented in Haidar Ahmad IA, Striegel AM. Determining the absolute, chemical-heterogeneity-corrected molar mass averages, distribution, and solution conformation of random copolymers. Anal Bioanal Chem 2010;396:1589–98.

[3] The original universal calibration paper by Benoit *et al.* was published a year earlier, in 1966, in the *Journal de Chimie Physique,* in French [35]. As noted by Benoit thirty years later, "Since it did not attract any attention I felt obliged to publish a short note as [33], which is the only paper referenced in the literature" [36].

as linear PS, it could then be applied, at the same experimental conditions as used to obtain the curve, to analytes with different chemistry and/or architecture, such as branched PS, PMMA, PVAc, and so on. The great advantage of the universal calibration concept was that the *M* averages and the MMD obtained by applying this curve were "absolute," that is, calibrant-independent. In the case just mentioned, the results for branched PS, PMMA, and PVAc would not be relative to linear PS, rather, they would be *the M* and MMD of these polymers. However, widespread application of the concept of universal calibration would have to wait until the introduction of a commercial viscometry detector for SEC, in the mid-1980s.

In 1985, Haney published two papers, "The differential viscometer. I. A new approach to the measurement of specific viscosities of polymer solutions" and "The differential viscometer. II. On-line viscosity detector for SEC" [37,38], With these, Viscotek Corp. (now Malvern) introduced a differential viscometer based on the Wheatstone bridge concept (this type of viscometer, shown in Fig. 10.7 is, in essence, the fluid flow equivalent of the classic Wheatstone bridge electrical circuit; its measurement of the specific viscosity η_{sp} of dilute polymer solutions is described in detail in Ref. [37] and in Section 9.5.2 of Ref. [2]).

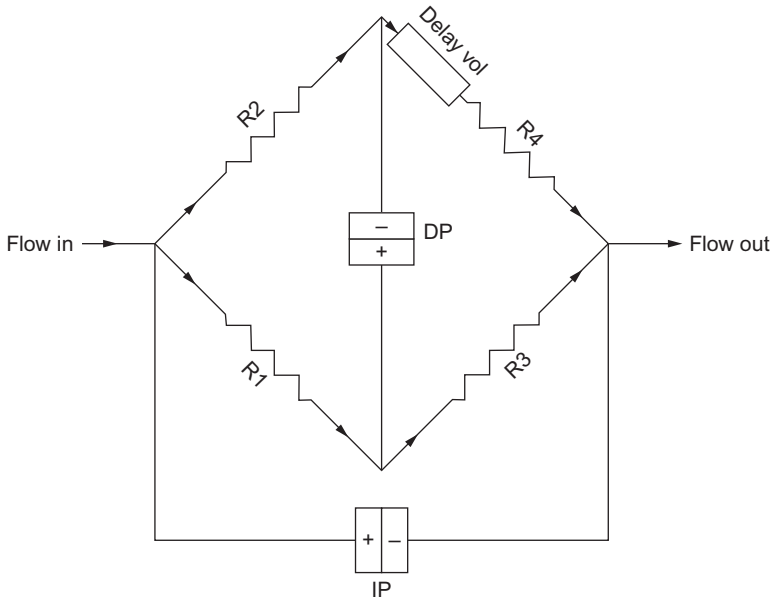

FIG. 10.7

Schematic of a Wheatstone bridge-type differential viscometer. R1–R4 refer to the different capillaries, DP is the differential pressure transducer, and IP is the inlet pressure transducer. Eluent from the SEC column enters the viscometer via the "Flow In" path.

Figure courtesy of Malvern Instruments.

In an SEC system with both DRI and viscometry (VISC) detectors, denoted SEC/VISC/DRI, at each elution slice the viscometer measures the specific viscosity and the refractometer measures the concentration c. Because intrinsic viscosity $[\eta]$ is defined as

$$[\eta] \equiv \lim_{c \to 0} \frac{\eta_{sp}}{c} \tag{10.17}$$

the ratio of the signals from the viscometer and the refractometer provides a continuous measure of intrinsic viscosity across the chromatogram. (As in all multidetector techniques discussed here, comparison among detector signals for a given elution slice presupposes correction for interdetector delay if the detectors are connected in series, or for eluent split ratio if the detectors are connected in parallel.) The availability of a robust, commercially available online viscometer allowed the implementation of the universal calibration concept of Benoit et al. on a widespread scale and, thus, the determination of absolute, calibrant-independent molar mass averages and distributions of a wide variety of polymers.

Given two polymers with the same monomeric repeat unit and with the same molar mass as each other (e.g., two polystyrenes of the same M), if one polymer is linear and the other is branched, the branched polymer will occupy a smaller hydrodynamic volume in solution than will the linear polymer. Consequently, the intrinsic viscosity of the branched polymer will be lower than that of its linear counterpart. The determination of intrinsic viscosity thus provided not only absolute M data, but also qualitative and even quantitative information of the branching status of the polymers and of how this status changes continually as a function of M, information not generally available from SEC experiments using only a single, concentration-sensitive detector.[4]

The universal calibration concept has proven itself quite robust, with few exceptions having been found over the years [40,41]. It has even been successfully applied to such architecturally extreme cases as rod-like polymers and dendrimers [42,43]. It should be noted, however, that a given universal calibration curve is valid only for a given column or column set, in a given solvent, at a given temperature, and at a given flow rate. If any of these parameters is changed (e.g., if a column is replaced, or if different solvent is to be used), a new universal calibration curve must be constructed. Because of this, coupled with the advent of online static light scattering (SLS) detectors (discussed next), the construction and application of universal calibration curves has experienced a decline in the last decade. As we shall see in Section 10.7, though, the online viscometer remains a powerful SEC detector, even when not being used for universal calibration purposes.

[4] The type of branching determined by on-line viscometry, and also by on-line light scattering detection, is long-chain branching, loosely defined as when branches are of a length comparable to, or a substantial fraction of, the length of the main macromolecular backbone [39].

10.6.2 SLS DETECTION

In an SLS experiment, measurement is made at a given angle θ of the light scattered by a dilute polymer solution in excess of that scattered by the neat solvent. This quantity is known as the *excess Rayleigh ratio* and given the symbol $\Delta R(\theta)$. The fundamental equation of SLS is known as the Rayleigh-Gans-Debye approximation, which is [2,44]

$$\frac{\Delta R(\theta)}{K^* c} = M_w P(\theta)\left[1 - 2A_2 c M_w P(\theta)\right] \tag{10.18a}$$

where

$$K^* = \frac{4\pi^2 n_0^2 \left(\partial n / \partial c\right)^2}{\lambda_0^4 N_A} \tag{10.18b}$$

and

$$\frac{1}{P(\theta)} = 1 + \frac{16\pi^2}{3\lambda^2} R_{G,z}^2 \sin^2\left(\frac{\theta}{2}\right) + \ldots \tag{10.18c}$$

In the above equations, N_A is Avogadro's number, n_0 the refractive index of the neat solvent at the experimental wavelength, λ_0 the vacuum wavelength of the incident radiation, λ the wavelength of the radiation in the medium ($\lambda \equiv \lambda_0/n_0$), c the concentration of polymer in solution, M_w the weight-average molar mass, $R_{G,z}$ the z-average radius of gyration (z-average root-mean-square radius), $P(\theta)$ the particle scattering factor, and $\partial n/\partial c$ is the specific refractive index increment of the solution. The A_2 term is the second virial coefficient, which characterizes the thermodynamic state of the solution (good, poor, or theta).[5]

At $\theta = 0°$, $P(\theta) = 1$ and Eq. (10.18a) reduces to:

$$\frac{\Delta R(\theta)}{K^* c} = M_w\left[1 - 2A_2 c M_w\right] \tag{10.19}$$

Given the dilute nature of the solutions being analyzed, and the additional dilutory effects of a chromatographic experiment, the approximation $A_2 \approx 0$ can often be made so that

$$\frac{\Delta R(\theta)}{K^* c} \approx M_w \tag{10.20}$$

The consequence of the above is that an SLS measurement at $\theta = 0°$ provides the absolute weight-average molar mass of the polymer without assumptions, models, or the need to construct a calibration curve.[6] Whereas measurements at $\theta = 0°$ are highly impractical, when $\theta = 7°$ then $P(\theta) = 0.98$ for macromolecules with $R_G \leq 150$ nm, with measurements made at angles closer to zero (i.e., at lower angles) providing for increased accuracy.

[5] The theta state is defined as the solvent/temperature condition at which $A_2 = 0$ for a dilute polymer solution, while at good conditions $A_2 > 0$ and at poor conditions $A_2 < 0$. This "theta" should not be confused with the scattering angle θ, to which it is unrelated. A_2 can usually be determined by employing the MALS photometer off-line, for so-called "batch mode" experiments; see Section 9.3.3 of Ref. [2] for details.

[6] At a fundamental level, the calculations rely on the relationship between index of refraction, dielectric constant, and polarizability, as given by the Clausius-Mosotti equation and Maxwell's theory of radiation.

In 1974, Ouano and Kaye wrote "Gel-permeation chromatography: X. Molecular weight detection by low-angle laser light scattering," in which they demonstrated the online coupling of SEC to a commercially available low-angle static light scattering (LALS) detector with a specially designed flow-through cell [45]. Measurement of scattered light was made at a narrow angular range of 4.1–4.8 degrees, and the system also used a DRI. As seen from Eq. (10.20):

$$M_w \propto \frac{\Delta R(\theta)}{c} \tag{10.21}$$

The SLS photometer measures $\Delta R(\theta)$ and the DRI measures concentration c at each slice i eluting from the SEC columns, so that the combination of detectors allows the M_w of each slice, $M_{w,i}$, to be determined. Because of the narrowness of the slices, they can be regarded as virtually monodisperse, so that $M_{w,i} \approx M_{n,i} \approx M_{z,i} \ldots \approx M_i$. Incorporating the M_i from SLS and the c_i from DRI into the Meyerhoff equation:

$$M_\beta = \frac{\sum_i c_i M_i^x}{\sum_i c_i M_i^{x-1}}, \quad \text{when} \quad x = 0, \beta = n; \quad \text{when} \quad x = 1, \beta = w; \quad \text{when} \quad x = 2, \beta = z \tag{10.22}$$

it can be seen how an SEC/SLS/DRI experiment allows the determination of the various M averages of a polymer, as well as of the polymer MMD, on an absolute basis and without the need to construct a calibration curve.

The above determinations of molar mass are performed most accurately by coupling SEC with LALS, the type of detector used by Ouano and Kaye in their experiments, because in LALS the data do not need to be corrected for angular effects. However, LALS provides no information about the size of the molecule (as, at $\theta = 0°$, the $R_{G,z}$ term vanishes from Eq. (10.18c)). Also, LALS experiments are notoriously sensitive to dust and other particulate matter (e.g., from the shedding of fines from column packing material), which scatters preferentially in the forward direction, that is, at low angles, rendering SEC/LALS data inherently noisy and plagued by spikes. It was these drawbacks of LALS (sensitivity to dust and no size information) that prompted the introduction of MALS detection.

In MALS, the scattered light is measured at a multiplicity of angles, simultaneously, using a number of individual photodiodes placed at discrete angular intervals around the MALS cell (an example of the placement of photodiodes around a commercial MALS cell is shown in Fig. 10.8A, whereas an example of the cell itself is shown in Fig. 10.8B). The combined results are then extrapolated to $\theta = 0°$ to obtain M_w, whereas the angular dependence of the scattered light (angular dissymmetry, due to intramolecular interference effects) is used to provide a measure of the size of the molecule, by way of the z-average radius of gyration $R_{G,z}$.[7] Fig. 10.9 shows a plot of

[7] Molecules that are small compared with λ, the wavelength of radiation in the medium, are considered near-isotropic scatterers, i.e., they scatter almost equally in all directions and, consequently, their R_G cannot be determined by MALS. A thumb rule is that the cut-off for accurate determination of R_G by MALS is when $R_G < \lambda/40$, where $\lambda \equiv \lambda_0/n_0$.

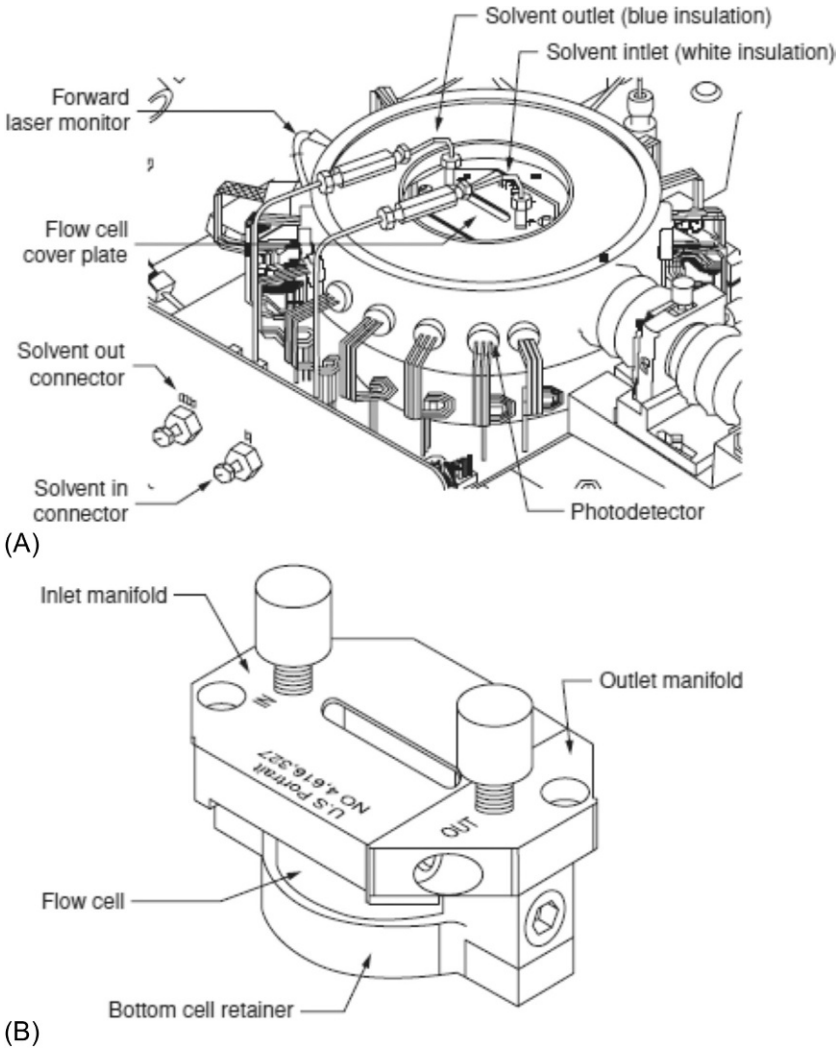

FIG. 10.8

(A) Read head of a commercial 18-angle MALS unit. (B) Flow cell assembly of 3-angle and 18-angle commercial MALS units.

Figures courtesy of Wyatt Technology Corp.

$K^*c/\Delta R(\theta)$ versus $\sin^2(\theta/2)$ for the slice eluting at the SEC peak apex, as measured by the 90 degree photodiode of the MALS detector, for the broad PS sample from Fig. 10.1. Each data marker represents the measurement from each photodiode of the MALS (the angular placement of the photodiodes is given by the numbers next to the individual data markers), with concentration c provided by the DRI subsequent to correction for interdetector delay.

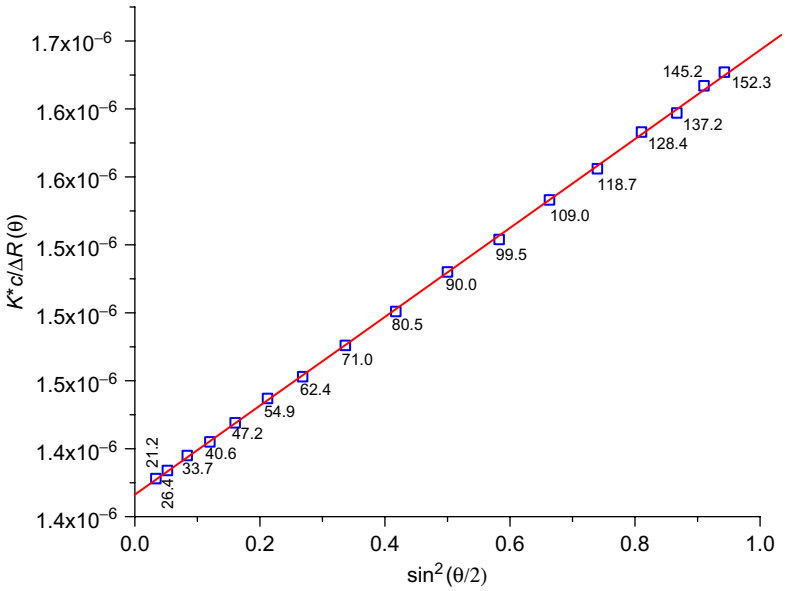

FIG. 10.9

Angular variation of scattered light intensity. Sample and experimental conditions as given in the legend for Fig. 10.1. Data are for SEC slice eluting at peak apex, as monitored by 90 degrees MALS photodiode, for which $M_w = 7.33 \times 10^5\,\mathrm{g\,mol^{-1}}$ and $R_{G,z} = 32\,\mathrm{nm}$. Error bars, representing instrumental standard deviation, are substantially smaller than data markers and, therefore, not shown. Solid line represents nonweighted, first-order linear fit to the data, with $r^2 > 0.999$. Numbers next to individual markers denote angle θ of measurement, in degrees (°), subsequent to correction for reflectance at the solvent-glass interface of the MALS cell.

Because, as described above, each slice eluting from the SEC column(s) is considered to be virtually monodisperse, coupling MALS and a concentration-sensitive detector to SEC allows calculation of the statistical averages and distribution of not just M, but also R_G. Fig. 10.10A shows the R_G distribution of the PS sample with MMD shown in Fig. 10.1. Given in Fig. 10.10B is the dependence of R_G on M. This so-called *conformation plot* has the ability to inform our knowledge of polymer architecture and/or dilute solution conformation. For example, in the present case, the slope of 0.53 is in the range expected for linear random coils at good solvent/temperature conditions, 0.5–0.6.

MALS detection for SEC was introduced in the mid-1980s [46]. Although it took some time for this detection method to gain acceptance, it is now considered the benchmark to which other determinations are compared. Current commercial offerings include systems which measure scattered light at 2, 3, 7, 8, 18, and 21 angles, simultaneously (the two latter systems actually provide measurements of, at the most, 17 and 20 angles when the MALS is connected to an SEC system or other type of separation device).

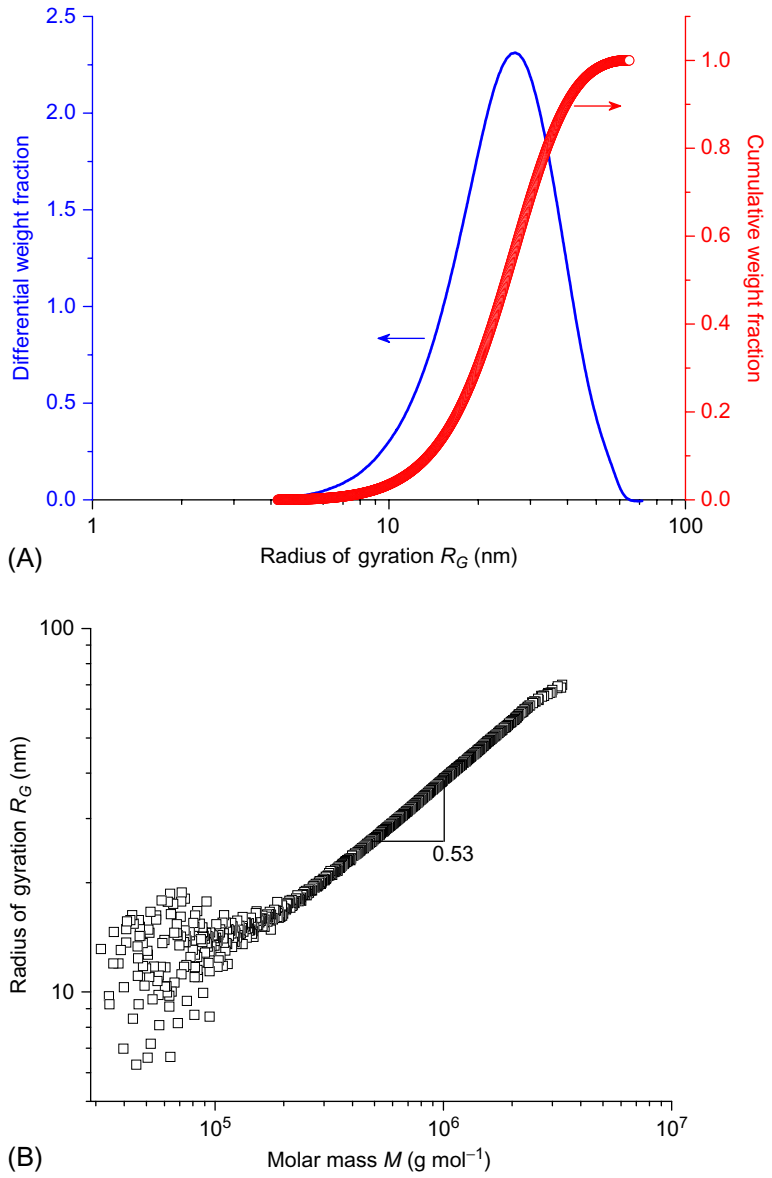

FIG. 10.10

(A) Differential (*solid blue line*) and cumulative (*open red circles*) distributions of R_G. Sample and experimental conditions as given in the legend for Fig. 10.1. Both distributions based on first-order polynomial fits to the experimental data. (B) Conformation plot for same sample as in (A), at same experimental conditions (for explanation of scatter at lower M values, see legend to Fig. 10.2). Slope is for a nonweighted, first-order linear fit of M data between $2\times10^5\,\mathrm{g\,mol^{-1}}$ and $3\times10^6\,\mathrm{g\,mol^{-1}}$, for which $r^2=0.999$.

As was the case with intrinsic viscosity, a (long-chain-)branched polymer will have a smaller R_G than will its linear counterpart of the same M and composed of the same monomeric repeat unit. As such, a comparison of the R_G of the linear and branched molecule, at the same M, can provide an indication of branching. With the MALS detector connected to an SEC system (or other suitable separation method) and assuming a suitable linear standard can be found,[8] branching can be determined across the chromatogram and, hence, across the MMD of the polymer. This determination of branching can be made fully quantitative by applying the theory developed by Bruno Zimm and Walter Stockmayer in their classic 1949 paper "The dimensions of chain molecules containing branches and rings" [47].

10.7 MULTIDETECTOR SEPARATIONS, PHYSICOCHEMICAL CHARACTERIZATION, 2D TECHNIQUES

Although multidetector SEC combining DRI, VISC, and MALS has been in use for at least the last two decades, the combination of detectors being used and the information obtained therefrom has certainly proliferated in this century [48,49]. The differential viscometer, for one, has grown beyond its role as a universal calibration tool and, like MALS, both these detectors are now also appreciated for the valuable architectural and conformational information they can provide when used together. The addition of quasielastic light scattering (QELS, also known as dynamic light scattering) detection, with the detector usually housed in the same unit as the MALS, added another tool to the arsenal of detectors used for characterizing physical aspects of macromolecules (consequently, these detectors are often referred to as "physical detectors"). In addition to long-chain branching information, these detectors can determine the persistence length, characteristic ratio, fractal dimension, and so on, of macromolecules across the MMD. Details of how this is done are given in Chapter 11 of Ref. [2].

Macromolecular behavior is often dictated not only by the topology but also by the chemistry of polymers, with observed conformational differences among physically similar species [50]. This is especially so in the case of copolymers, where the relative amounts of the different monomers, and the arrangement of these monomers both within the chain and across the MMD, influences processing, end-use, and dilute solution properties [51]. To better understand the underlying basis of this behavior, results from the above physical detectors have been augmented by the addition of detection by mass spectrometry; ultraviolet, infrared, fluorescence, and nuclear magnetic resonance spectroscopy; conductivity;

[8] The requirements for accurately performing long-chain branching calculations, including the suitability qualifications for a linear standard, are described in Section 11.2 of Ref. [2] and in Ref. [39].

and so on. When used in conjunction with MALS and a suitable concentration-sensitive detector, the latter detectors (often referred to as "chemical detectors") can measure how the average ratio of the various monomers in a copolymer changes as a function of molar mass, a datum known as *chemical heterogeneity*, or how tacticity or polyelectrolytic charge changes as a function of M. Ludlow et al. have combined various chemical detectors, namely, UV, ^{1}H NMR, ESI-MS, and off-line continuous FT-IR in the study of polymer additives [52], whereas Striegel and colleagues have applied quadruple- and quintuple-detector SEC with a combination of physical and chemical detectors to the study of copolymers and blends [34,53]. For example, using SEC/MALS/QELS/VISC/UV/DRI, with all detectors online, Rowland and Striegel determined the chemical heterogeneity in a poly(acrylamide-*co*-*N,N*-dimethyl acrylamide) copolymer, the chemical heterogeneity-corrected molar mass averages and distribution of the copolymer, its dilute solution conformation, and how this conformation changed across the MMD, as well as the physicochemical basis for the observed changes, all in a single analysis [53].

Whereas many characteristics of homo- and copolymers can be characterized by multidetector SEC, a number of other separation techniques provide complementary information [54]. Examples are the chemical composition distribution (CCD) of copolymers, obtained via the so-called "interactive" macromolecular separation methods such as gradient polymer elution chromatography (GPEC) or liquid adsorption chromatography at the critical condition (LACCC) [55–57]. Alternatively, techniques such as hydrodynamic chromatography or field-flow fractionation may be used to study molecules or particles that are either too large or too fragile to be analyzed successfully by SEC [20,21,26,27,58]. A corollary of these needs is that, for a more complete understanding of complex polymers (understood as polymers with distributions in more than one property) and blends, it is necessary to couple SEC to other types of separation methods. In these 2D-LC separations, a polymer with distributions in both molar mass and chemical composition may be analyzed by e.g., GPEC × SEC, to determine the combined CCD × MMD of the macromolecule. Fig. 10.11 shows the results of an LACCC × SEC analysis of a block copolymer of PMMA and poly(isobornyl acrylate) or PiBoA. The contour plot shows the presence not only of the PMMA-*b*-PiBoA block copolymer, but also of the remaining PiBoA homopolymer that was used in the copolymer synthesis. Relative abundances are given by the scale bar and, more informatively, by the three-dimensional rendering of each peak, to the right of the 2D chromatogram.

Recent reviews of 2D-LC of polymers include Refs. [60,61], whereas the theory and applications of 2D-LC with SEC as one of the dimensions are treated in Chapter 14 of Ref. [2]. It can safely be said that multidimensional, multidetector macromolecular separations will be *the* growth area in polymer chromatography in upcoming years, due to the power of this group of techniques both with respect to peak capacity as well as to the wealth of information they can provide about the physicochemical phase space occupied by complex polymers and blends.

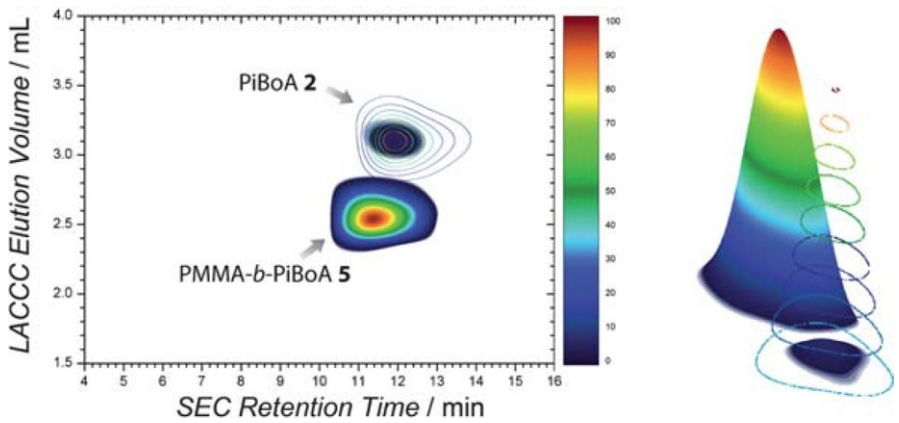

FIG. 10.11

2D LACCC × SEC chromatogram of PMMA-*b*-PiBoA, showing the remaining PiBoA homopolymer after the synthesis of the block copolymer. Relative abundances are given by the scale bar and by the three-dimensional rendering of each peak, to the right of the 2D chromatogram. See Ref. [59] for experimental details.

Reprinted with permission from reference Inglis AJ, Barner-Kowollik C. Visualizing the efficiency of rapid modular block copolymer construction. Polym Chem 2011;2:126–36. DOI: 10.1039/C0PY00189A.

10.8 CONCLUSIONS

SEC can be said to have "come of age" in the 1980s with the ability to determine absolute *M*, as imparted by online SLS and viscometric detection (the latter because it permitted construction of universal calibration curves), using robust, commercially available detectors. The next decade was chiefly governed by triple-detector methods involving MALS, VISC, and DRI to determine a number of physical properties, with many studies involving the measurement (with varying levels of accuracy) of long-chain branching across the MMD of both natural and synthetic polymers. During this period, the coupling of SEC to chemical detectors also grew. Today, multidetector SEC experiments may involve three, four, and even five detectors, all online, to characterize a wide range of physicochemical properties such as *M* averages and distributions, chemical and sequence-length heterogeneity, long- and short-chain branching, fractal dimension and persistence length, and more. With the growing knowledge of the power of SEC has also come the realization of many of its limitations, especially when a more complete characterization of complex polymers and blends is desired [2,62]. To deconvolute from each other the multiple physical and chemical distributions that may be present in these types of materials, 2D separations are usually necessary, and SEC has found a central role in these methods, as well. Indeed, it is in the acceptance and popularization of multidetector, multidimensional techniques that macromolecular separation science can be expected to grow and to demonstrate its full power in the upcoming years. This is likely to be accompanied

by advances in the synthesis of stationary phases specifically tailored for interactive macromolecular separations, and by continued computer modeling and simulations of the various distributions and heterogeneities present in copolymers and related materials [43,51,63].

ACKNOWLEDGMENT AND DISCLAIMER

The author is most grateful to Dr. Philip J. Wyatt for insightful discussions on the early days of interfacing MALS to separation systems in general, and to SEC in particular. The identification of certain commercial equipment, instruments, or materials does not imply recommendation or endorsement by the National Institute of Standards and Technology. These identifications are made only in order to specify the experimental procedures in adequate detail.

REFERENCES

[1] Rudin A. The elements of polymer science and engineering. New York: Academic Press; 1982.
[2] Striegel AM, Yau WW, Kirkland JJ, Bly DD. Modern size-exclusion liquid chromatography. 2nd ed. New York: Wiley; 2009.
[3] Moore JC. Gel permeation chromatography. I. A new method for molecular weight distribution of high polymers. J Polym Sci A 1964;2:835–43.
[4] Wheaton RM, Bauman WC. Non-ionic separations with ion exchange resins. Ann N Y Acad Sci 1953;57:159–76.
[5] Porath J, Flodin P. Gel filtration: a method for desalting and group separation. Nature 1959;183:1657–9.
[6] Striegel AM. Separation science of macromolecules: what is the role of multidetector size-exclusion chromatography? Chapter 1, In: Striegel AM, editor. Multiple detection in size-exclusion chromatography. ACS Symposium Series, vol. 893. Washington, DC: American Chemical Society; 2005. p. 2.
[7] Moore JC. Gel permeation chromatography: its inception. J Polym Sci C 1968;21:1–3.
[8] Ouano AC. Gel-permeation chromatography. VII. Molecular weight determination of GPC effluents. J Polym Sci A-1 1972;10:2169–80.
[9] McDonald PD. Waters corporation: fifty years of innovation in analysis and purification. Chem Heritage 2008;33–7. Summer.
[10] McDonald PD. James Waters and his liquid chromatography people: a personal perspective. www.waters.com.
[11] Striegel AM. Anomeric configuration, glycosidic linkage, and the solution conformational entropy of O-linked disaccharides. J Am Chem Soc 2003;125:4146–8 (see Erratum in J. Am. Chem. Soc. 2004:126:4740).
[12] Boone MA, Striegel AM. Influence of anomeric configuration, degree of polymerization, hydrogen bonding, and linearity versus cyclicity on the solution conformational entropy of oligosaccharides. Macromolecules 2006;39:4128–31.
[13] Boone MA, Nymeyer H, Striegel AM. Determining the solution conformational entropy of O-linked oligosaccharides as quasi-physiological conditions: size-exclusion chromatography and molecular dynamics. Carbohydr Res 2008;343:132–8.

[14] Buley TD, Striegel AM. Relation between the Δ2 effect and the solution conformational entropy of aldohexoses and select methyl glycosides. Carbohydr Polym 2010;79:241–9.
[15] Striegel AM, Boone MA. Influence of glycosidic linkage on solution conformational entropy of oligosaccharides: Malto- vs. isomalto- and cello- vs. laminarioligosaccharides. Biopolym 2011;95:228–33.
[16] Richard DJ, Striegel AM. The obstruction factor in size-exclusion chromatography. 1. The intraparticle obstruction factor. J Chromatogr A 2010;1241:7131–7.
[17] Little JN, Waters JL, Bombaugh KJ, Pauplis WJ. Fast gel-permeation chromatography. I. A study of operational parameters. J Polym Sci A-2 1969;7:1775–83.
[18] Yau WW, Malone CP, Fleming SW. The equilibrium distribution coefficient in gel permeation chromatography. J Polym Sci Part B Polym Lett 1968;6:803–7.
[19] Striegel AM. Thermodynamic equilibrium of the solute distribution in size-exclusion chromatography. J Chromatogr A 2004;1033:241–5.
[20] Striegel AM. Hydrodynamic chromatography: packed columns, multiple detectors, and microcapillaries. Anal Bioanal Chem 2012;402:77–81.
[21] Striegel AM, Brewer AK. Hydrodynamic chromatography. Annu Rev Anal Chem 2012;5:15–24.
[22] Uliyanchenko E, van der Wal S, Schoenmakers PJ. Deformation and degradation of polymers in ultra-high-pressure liquid chromatography. J Chromatogr A 2011;1218:6930–42.
[23] Striegel AM. Longitudinal diffusion in size-exclusion chromatography: a stop-flow size-exclusion chromatography study. J Chromatogr A 2001;932:21–31.
[24] Striegel AM. Observations regarding on-column, flow-induced degradation during SEC analysis. J Liq Chromatogr Relat Technol 2008;31:3105–14.
[25] Striegel AM, Isenberg SL, Côté GL. An SEC/MALS study of alternan degradation during size-exclusion chromatographic analysis. Anal Bioanal Chem 2009;394:1887–93.
[26] Isenberg SL, Brewer AK, Côté GL, Striegel AM. Hydrodynamic versus size exclusion chromatography characterization of alternan and comparison to off-line MALS. Biomacromolecules 2010;11:2505–11.
[27] Brewer AK, Striegel AM. Characterizing string-of-pearls colloidal silica by multidetector hydrodynamic chromatography and comparison to multidetector size-exclusion chromatography, off-line multiangle static light scattering, and transmission electron microscopy. Anal Chem 2011;83:3068–75.
[28] Giddings JC. Dynamics of chromatography. New York: Marcel Dekker; 1965.
[29] Giddings JC. Unified separation science. New York: Wiley; 1991.
[30] Snyder LR, Kirkland JJ, Dolan JW. Introduction to modern liquid chromatography. 3rd ed. New York: Wiley; 2010.
[31] Karger BI, Snyder LR, Horvath C. An introduction to separation science. New York: Wiley; 1973.
[32] Yau WW, Kirkland JJ, Bly DD, Stoklosa HJ. Effect of column performance on the accuracy of molecular weights obtained from size exclusion chromatography (gel permeation chromatography). J Chromatogr 1976;125:219–30.
[33] Grubisic Z, Rempp P, Benoit H. A universal calibration for gel permeation chromatography. J Polym Sci Polym Lett Ed 1967;5:753–9.
[34] Haidar Ahmad IA, Striegel AM. Determining the absolute, chemical-heterogeneity-corrected molar mass averages, distribution, and solution conformation of random copolymers. Anal Bioanal Chem 2010;396:1589–98.

[35] Benoit H, Grubisic Z, Rempp P, Decker D, Zilliox J-G. Étude par chromatographie en phase liquid de polystyrènes linéaires et ramifiés de structures connues. J Chim Phys 1966;63:1507–14.
[36] Benoit HC. Reflections on "A universal calibration method for gel permeation chromatography". J Polym Sci 1967;5:753, by Z. Grubisic, P. Rempp, and H. Benoit, J Polym Sci B Polym Phys 1996;34:1703–1704.
[37] Haney MA. The differential viscometer. I. A new approach to the measurement of specific viscosities of polymer solutions. J Appl Polym Sci 1985;30:3023–36.
[38] Haney MA. The differential viscometer. II. On-line viscosity detector for size-exclusion chromatography. J Appl Polym Sci 1985;30:3037–49.
[39] Striegel AM. Long-chain branching macromolecules: SEC analysis. In: Cazes J, editor. Encyclopedia of chromatography. 3rd ed. New York: Taylor & Francis; 2010. p. 1417.
[40] Dubin PL, Principi JM. Failure of universal calibration for size-exclusion chromatography of rodlike macromolecules versus random coils and globular proteins. Macromolecules 1989;22:1891–6.
[41] Pannell J. Gel permeation chromatography: the behavior of polystyrenes with long-chain branching. Polym 1972;13:277–82.
[42] Temyanko E, Russo PS, Ricks H. Study of rodlike homopolypeptides by gel permeation chromatography with light scattering detection: Validity of universal calibration and stiffness assessment. Macromolecules 2001;34:582–6.
[43] Striegel AM, Plattner RD, Willett JJ. Dilute solution behavior of dendrimers and polysaccharides: SEC, ESI-MS, and computer modeling. Anal Chem 1999;71:978–86.
[44] Wyatt PJ. Light scattering and the absolute characterization of macromolecules. Anal Chim Acta 1993;272:1–40.
[45] Ouano AC, Kaye W. Gel-permeation chromatography, X. Molecular weight detection by low-angle laser light scattering. J Polym Sci Polym Chem Ed 1974;12:1151–62.
[46] (a) Wyatt PJ, Jackson C, Wyatt GK. Absolute GPC determinations of molecular weights and sizes from light scattering. Am Lab 1988;20:86–9. (b)Wyatt PJ, Hicks DL, Jackson C, Wyatt GK. Absolute GPC determinations of molecular weights and sizes. Am Lab 1988;20:108–11.
[47] Zimm BH, Stockmayer WH. The dimensions of chain molecules containing branches and rings. J Chem Phys 1949;17:1301–14.
[48] Multiple detection in size-exclusion chromatography. In: Striegel AM, editor. ACS Symposium Series, 893. Washington, DC: American Chemical Society; 2005.
[49] Striegel AM. Multiple detection in size-exclusion chromatography of macromolecules. Anal Chem 2005;77:104A–13A.
[50] Haidar Ahmad IA, Striegel AM. Influence of second virial coefficient and persistence length on dilute solution polymer conformation. Anal Bioanal Chem 2011;399:1515–21.
[51] Haidar Ahmad IA, Striegel DA, Striegel AM. How does sequence length heterogeneity affect the dilute solution conformation of copolymers? Polym 2011;52:1268–77.
[52] Ludlow M, Louden D, Handley A, Taylor S, Wright B, Wilson ID. Size-exclusion chromatography with on-line ultraviolet, proton nuclear magnetic resonance and mass spectrometric detection and on-line collection for off-line Fourier transform infrared spectroscopy. J Chromatogr A 1999;857:89–96.
[53] Rowland SM, Striegel AM. Characterization of copolymers and blends by quintuple-detector size-exclusion chromatography. Anal Chem 2012;84:4812–20.
[54] Striegel AM. Separation science of macromolecules. Anal Bioanal Chem 2011;399:1399–400.

[55] Striegel AM. Determining the vinyl alcohol distribution in poly(vinyl butyral) using normal-phase gradient polymer elution chromatography. J Chromatogr A 2002;971:151–8.
[56] Striegel AM. Determining and correcting "moment bias" in gradient polymer elution chromatography. J Chromatogr A 2003;996:45–51.
[57] Philipsen HJA. Determination of chemical composition distribution in synthetic polymers. J Chromatogr A 2004;1037:329–50.
[58] Podzimek S. Light scattering, size exclusion chromatography and asymmetric flow field flow fractionation. New York: Wiley; 2011.
[59] Inglis AJ, Barner-Kowollik C. Visualizing the efficiency of rapid modular block copolymer construction. Polym Chem 2011;2:126–36. http://dx.doi.org/10.1039/C0PY00189A.
[60] Berek D. Two-dimensional liquid chromatography of synthetic polymers. Anal Bioanal Chem 2010;396:421–41.
[61] Baumgaertel A, Altuntaş E, Schubert US. Recent developments in the detailed characterization of polymers by multidimensional chromatography. J Chromatogr A 2012;1240:1–20.
[62] Berek D. Size exclusion chromatography—a blessing and a curse of science and technology of synthetic polymers. J Sep Sci 2010;33:315–35.
[63] Dong S, Striegel AM. Monte Carlo simulation of the sequence length and junction point distributions in random copolymers obeying Bernoullian statistics. Int J Polym Anal Charact 2012;17:247–56.